

Systematics of Coulomb excitation with limited effects from nuclear distortion*

Da Hsuan Feng†

Department of Physics, University of Texas at Austin, Austin, Texas 78712

A. R. Barnett

Department of Physics, Schuster Laboratory, University of Manchester, Manchester, U.K. M13 9PL

L. J. B. Goldfarb

Department of Theoretical Physics, University of Manchester, Manchester, U.K. M13 9PL

(Received 10 September 1975)

A wide-ranging survey has been made of (α, α') scattering from various target nuclei. Particular emphasis was given to determination of the departures of the cross section from Coulomb excitation, which are due mainly from nuclear interaction. The energy range in this study covers the region from the Coulomb barrier and downwards. Calculations were performed to first order only via the distorted-wave Born approximation method and the usual collective model was assumed. It is found that the inelastic scattering is more sensitive to the nuclear distortion than the elastic scattering, which conforms with results of recent experiments. A discussion is given of the Igo ambiguity in elastic and inelastic scattering near the barrier.

NUCLEAR REACTIONS Elastic and inelastic α -particle scattering on medium- and heavy-weight nuclei, Coulomb-nuclear interference, Coulomb barrier, safe distance, multipolarities, Igo ambiguities, strong absorption radius.

I. INTRODUCTION

The influence of the nuclear interaction between the projectile and the target during inelastic scattering has not been studied systematically in the bombarding energy range below the Coulomb barrier. Coulomb excitation theories,¹⁻³ and especially those describing the reorientation effect (due to static quadrupole moments of the nuclei) or other higher order processes,⁴ specifically assume that there is no interaction between the two charges aside from the electromagnetic field; thus deviations from the first-order calculations are attributed to the effects of static quadrupole moment⁴ and of higher moments. It is consequently of great interest to establish quantitatively that nuclear effects do not upset the validity of the Coulomb-excitation approximations. We have completed a series of calculations designed to reveal the degree of importance of nuclear effects in some Coulomb-excitation experiments. These are the (α, α) and (α, α') reactions on the target nuclei ¹⁵²Sm, ²⁰⁹Pb, and ²³⁴U as a function of bombarding energy.

Recently a number of α -scattering experiments have been performed whose object has been to measure nuclear and Coulomb interference effects both in the Coulomb barrier region and at a sufficiently low energy that nuclear effects are negligible. The deformed targets ^{152,154}Sm and ¹⁸⁶W,⁵ ¹⁵⁴Sm, ¹⁶⁶Er and ¹⁸²W,⁶ ¹⁶⁸Er and ^{184,186}W,⁷

and eight rare-earth isotopes from ¹⁵²Sm to ¹⁷⁴Yb⁸ have been studied by this method and in each case quantal coupled-channel calculations have been made. Nuclear and Coulomb effects are both included in such calculations.

The "safe energy," which is the energy below which nuclear effect is negligible, is defined in terms of a minimum distance between the two nuclei in a head-on collision

$$S = (Z_1 e)(Z_2 e)E^{-1} - r_0(A_1^{1/3} + A_2^{1/3}), \quad (1)$$

where Ze and A are the charge and mass number of the particles, E is their relative center-of-mass kinetic energy, and r_0 is a nuclear radius parameter. Various attempts have been made to estimate values for S for which nuclear effects are indeed negligible; de Boer and Eichler⁴ proposed $S > 3$ fm with $r_0 = 1.25$ fm, and it was soon recognized experimentally that this choice was not stringent enough; Cline *et al.* showed that the condition $S > 5.1$ fm⁹; later¹⁰ $S > 6$ fm, is necessary, while the Purdue group¹¹ demonstrated that with r_0 set equal to 1.6 fm, then $S > 3$ fm. It is important to realize that these experimental tests all refer to $L = 2$ excitation with projectiles of mass 16 to 32 incident of medium-mass targets. Thus the use of these criteria for widely different mass regions will lead to widely different predictions for values of $S(E)$.

The terms "safe" and "negligible" are clearly subjective in nature. We might arbitrarily adopt

a criterion that a nuclear effect is significant or nonnegligible if the alteration in the calculated differential cross section is at least 5% of the higher-order Coulomb excitation being considered. Our purpose is to establish the usefulness of such criteria, at least for the cases we consider. We also wish to exhibit the systematic features which are of major importance, such as the multipolarity of the transition and the excitation energy. We will demonstrate the danger in making estimates of nuclear effects simply by noting observed deviations from Rutherford scattering.

Our approach is to perform exact calculations within the framework of the distorted-wave Born approximation (DWBA) for the Coulomb-excitation term by including sufficient partial waves (up to 700 at present)^{12,25} and by extending the radial integrations where necessary to several hundred femtometers. The properties of the code PATWEN,¹² which was written by two of us (DHF and ARB) for this purpose, are outlined in Sec. II; the code can be used to calculate Coulomb excitation to first order with and without nuclear effects and hence it will directly reveal their relative importance. The results can also be used to test symmetrization procedures in the semiclassical calculations of Coulomb excitation.^{1-3,13} There is much current activity in the field of semiclassical heavy-ion reactions calculations¹⁴ where important approximations have to be made in order to render the calculations tractable and to provide physical insight; such approaches can be directly compared with our exact first-order solution. For our purposes the "Coulomb barrier" is that incident energy which equals the sum of the nuclear and Coulomb potentials for an $l=0$ partial wave. How effective a barrier to nuclear effects this is will be seen in the following.

The code is not restricted in energy (apart from being nonrelativistic) and it can be readily used for cases of high incident energy where Coulomb excitation is of minor importance compared to nuclear excitation. Of more interest, however, is the region which straddles the Coulomb barrier,¹⁵ and extends above it, in which the Coulomb-nuclear interference phenomenon is most pronounced, since there the contributions of the two excitation mechanisms are similar in magnitude. Much experimental work has recently appeared which focuses attention on this region for both light and heavy ions and for many cases the DWBA provides a reliable method of calculation.¹⁵⁻¹⁹

This paper restricts itself to a study of (α, α') reactions on samarium and uranium for multipolarities of $L=2$ and $L=4$ (the first-order part

only) and on lead for $L=3$. All these cases have been the subject of recent experimental study by Coulomb excitation^{5,20-23} so that our results are directly relevant to these experiments. Section III discusses typical angular distributions for elastic and inelastic scattering.

Section IV treats the samarium results, Sec. V the lead results, and Sec. VI the uranium results. Our main conclusions are contained in Figs. 8, 10, and 11, which give the percentage deviation of the inelastic scattering from the Coulomb excitation (CE) value [more strictly the distorted wave CE (DWCE) value] as a function of energy for each multipolarity. This quantity displays quantitatively the meaning of the safe energy. A further conclusion is to suggest a generalized Igo ambiguity criterion for inelastic scattering and hence to point out the large uncertainties which probably should be attached to nuclear deformation parameters which are deduced from βR values used in the analysis. This point is taken up in the next section.

II. THEORY

A. Formulation

In our study we have adopted the conventional collective-model description of the nuclear form factor, since it represents a convenient approximation for our purpose, which is to demonstrate quantitatively the progressive weakening of nuclear effects as the bombarding energy is decreased. Thus, neither the precise optical potentials nor the precise shape of the nuclear form factor are crucial to our conclusions. The standard expression²⁶⁻²⁸ for the inelastic scattering of α particles entails the calculation of matrix elements.

$$\langle \chi^-(\vec{k}, \vec{r}) | F_L^C(\hat{r}) Y_{LM} | \chi^+(\vec{k}, \vec{r}) \rangle$$

for Coulomb excitation

and

$$\langle \chi^-(\vec{k}, \vec{r}) | F_L^N(\hat{r}) Y_{LM}(r) | \chi^+(\vec{k}, \vec{r}) \rangle$$

for nuclear excitation.

The nuclear form factor $F_L^N(r)$ for an initial target spin of zero is

$$F_L^N(r) = \beta_L^N R dU(r)/dr, \quad (2)$$

where β_L^N is the optical potential deformation parameter and R the halfway radius of the optical potential $U(r)$. In the case where the real and imaginary parts of $U(r)$ have the same radial form then

$$U(r) = (V + iW) \{1 + \exp[(r - r_0)/a]\}^{-1}, \quad (3)$$

while for the case where the imaginary well has a different geometry we choose

$$F_L^N(r) = \beta_R R dV(r)/dr + i\beta_I R' dW(r)/dr. \quad (4)$$

In a first-order treatment all the deformation information concerning the nucleus is contained in the parameters β_L^N , β_R , or β_I (strictly speaking, this information is in the form $\beta_R R/a$ and $\beta_I R'/a'$ — see Sec. II B).

The Coulomb form factor is

$$F_L^C(r) = 4\pi Z_1 e |B(EL; 0 \rightarrow L)|^{1/2} (2L+1)^{-1} r^{-L-1}, \quad r > R_C, \quad (5)$$

$$= \beta_L^C 3Z_1 Z_2 e^2 (2L+1)^{-1} r^L R_C^{-L-1}, \quad r \leq R_C. \quad (6)$$

The parameter R_C is the charge radius, i.e., the radius of a uniform spherical charge distribution. It is not a critical parameter in our calculations since the energy range is low enough that the interaction is insensitive to this region of space; we have chosen it to be the electron scattering radius $1.20(A_2)^{1/3}$. The insensitivity disappears when heavier ions are used as projectiles and the results can be crucially dependent²⁹ on the choice of R_C . In such cases it seems most reasonable to use as the interaction radius the sum of the radii of projectile and target. The electric transition matrix element $|B(EL; 0 \rightarrow L)|^{1/2}$ is related to the charge-density deformation parameter β_L^C by relations (5) and (6):

$$|B(EL; 0 \rightarrow L)|^{1/2} = 3Z_2 e R_C^L \beta_L^C 4\pi. \quad (7)$$

Under the assumption that the charge deformation β_L^C is the same as the potential deformation β_L^N , we use $\beta_L^C = \beta_L^N$. For our purposes we need inquire no deeper. Similarly, the details of the form factor and the implicit assumptions contained in it are most important when relating the data to nuclear properties.

Program PATIWEN evaluates the radial matrix elements for CE by direct integration.^{12,24} The computational time required in these calculations is directly related to a specified accuracy; also, the time will decrease as the multipolarity decreases and as the excitation energy increases. Lower L values require more extensive radial integration to handle the r^{-L-1} factor while smaller ξ values (small energy loss between initial and final channels) imply good matching between the Coulomb wave functions and hence a slow decrease in the magnitude of the $M_{l,l'}^L$ (see Ref. 12 for the definition of this quantity) with l value. Examples are shown in Figs. 1 and 2 for $L=2$; the matrix elements have decreased by two orders of magnitude at $l=200$, and then decrease at a much

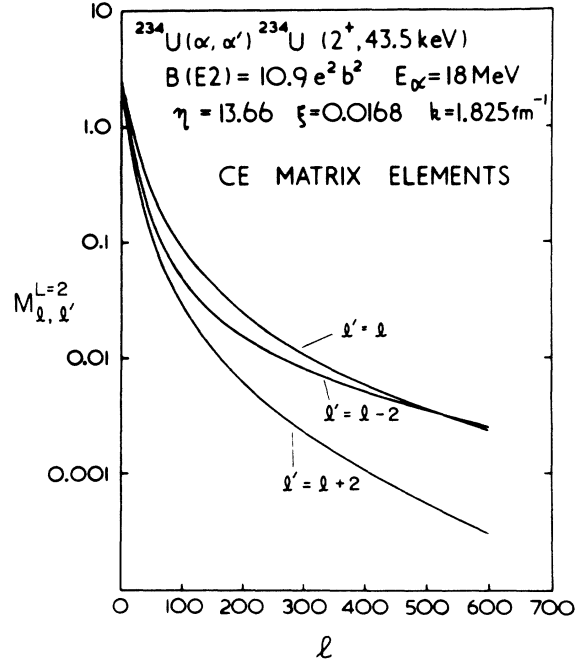


FIG. 1. Plot of the matrix element $M_{l,l'}^{L=2}$ (see text for definition) versus l value. The coupling between l and l' is governed by the Clebsch-Gordan coefficient $(l'l'0|20)$ which results in three curves as shown.

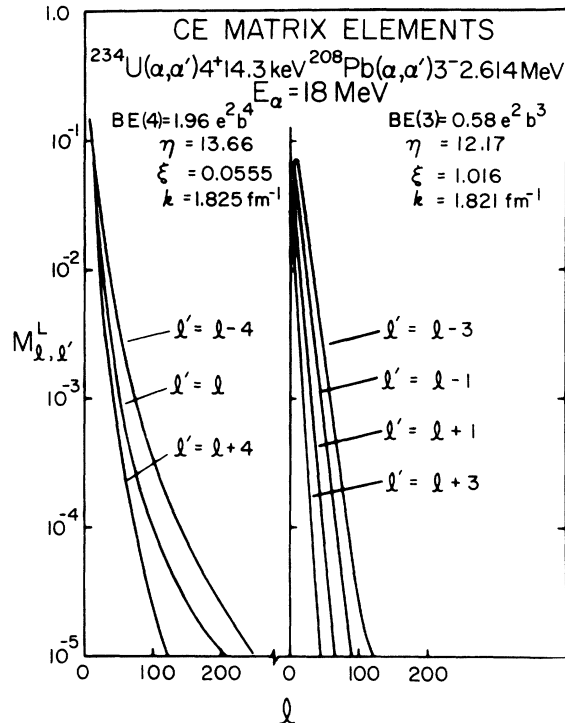


FIG. 2. Plot of the matrix elements $M_{l,l'}^{L=4}$ and $M_{l,l'}^{L=3}$ versus l value. The coupling between l and l' is governed by the Clebsch-Gordan coefficient $(l'l'0|L0)$. However, for $L=4$ only $l' = l \pm 4$ and $l' = l$ are displayed.

slower rate which is a factor of 10 in 300 or 400 l values. The $L=4$ matrix elements have decreased by more than four orders of magnitude at $l=200$. The $L=3$ case is much easier computationally because of the higher multipolarity and, for ^{208}Pb , the very large mismatch between channels ($\xi=1.0$), leading directly to a small cross section.

B. Igo ambiguity in elastic and inelastic α scattering

By the term Igo ambiguity we understand the statement that only the tails of the nuclear potentials are important in determining low and medium energy α scattering since these projectiles are strongly absorbed and are thus insensitive to the nuclear interior. Igo deduced this result³⁰ from his analysis of early elastic scattering data and the concept has remained an important one. It is based on the strong-absorption property of α particles and will thus, presumably, hold as well for heavy ions. The nuclear potential is almost invariably parametrized in a Woods-Saxon form, which at large distances ($r > R + 5a$) becomes

$$V(r) = V_0 e^{-(r-R)/a} \equiv V_0 e^{R/a} e^{-r/a}. \quad (8)$$

Thus, potentials equivalent in the tail region have equal values of the quantity

$$X_{\text{Igo}}(a) \equiv V_0 e^{R/a} \quad (9)$$

and have equal values of the diffuseness.

It is a well-known feature of the analysis of elastic scattering by strongly absorbed particles that the magnitude of the real potential is a well-determined quantity in the neighborhood of a point in the surface, at $r=R_s$, so that the potentials with different values of diffuseness intersect at or near this radius. Examples can be found in papers by Cage, Cole, and Pyle,³¹ Jackson and Morgan,³² Mailandt, Lilley, and Greenlees,³³ and Barnett and Lilley.³⁴ The results are for ^3He and ^4He scattering on medium mass nuclei and also for ^4He on ^{208}Pb and ^{209}Bi at Coulomb barrier energies. A complete discussion of the possible choices for R_s is given by Fernandez and Blair,³⁵ and Rawitscher³⁶ also investigates these ambiguities in great detail. This feature, indeed, has frequently been adopted as the criterion for strong absorption. We then have as a more precise statement of the general Igo ambiguity: *equivalent potentials for elastic scattering are those for which the real potential is the same for some radius in the surface, and not for all radii in the tail of the potential (which implies the same diffuseness). At this radius, labeled R_s , we have*

$$V(R_s) = X_{\text{Igo}} \equiv V_0 e^{R/a} e^{-R_s/a} = \text{constant}, \quad (10)$$

and this equation should express the complete a dependence of the quantity $X_{\text{Igo}}(a)$. A part of this paper is concerned with the consequences of Eq. (9), namely the continuous V_0 - R Igo ambiguity for fixed diffuseness; the consequences of Eq. (10) are touched on in Sec. VII together with possible choices for R_s .

From the assumptions of the collective model²⁶ the real form factor for inelastic scattering can be derived from the real potential as

$$(\beta_L^N R) a^{-1} V_0 e^{R/a} e^{-r/a} = (\beta_L^N R) a^{-1} V(R_s) \quad (11)$$

at large radii, and so an Igo ambiguity involving the quantity $a^{-1} X_{\text{Igo}}$ or $a^{-1} X_{\text{Igo}}(a)$ might well be anticipated. This expectation we shall show to be well justified and it has the following important consequence^{37,38}: For potentials with a fixed value of the diffuseness a , the central radius R can be varied over a noticeable range, in some cases from +5% to -15%, with almost complete compensation being provided by a corresponding change in V_0 ; both the predicted elastic scattering and the inelastic scattering (provided β_L^N is varied to keep $\beta_L^N R a^{-1}$ constant) are unaltered to any significant degree. Thus deductions concerning the magnitude of the "nuclear deformation" parameter β_L^N on the assumption that R is a known quantity may be suspect to the order of 15%-20%.

This ambiguity can be looked at from two points of view. One of these emphasizes the simple dependence of differential cross section on only the tails of the nuclear potentials. Few parameters are therefore needed to account for the nuclear interaction. The other viewpoint concentrates on limitations in the delineation of the potentials and on the uncertainties associated with the extension of the same potentials to inelastic scattering.

The above conclusions are certainly the case in the energy range studied in this paper. At a sufficiently high energy the radial curvature of the potentials will be important and so will details of the imaginary potential. Consequently the range of the Igo ambiguity will become more restricted. Jackson and Morgan³² have indeed demonstrated at higher energies that the acceptable variation of a is very small.

For the imaginary potential we might also expect an Igo ambiguity to hold, at least to some more limited extent, since the functions of the real and imaginary potentials in α scattering are different (see, e.g., Ref. 34). The surface of the real potential largely determines the reflection coefficients and regulates the amount of flux which penetrates into the interior, whereas the strength controls the amount of this flux which is absorbed. Consequently, surface-peaked and volume imaginary potentials a^{-1} may drastically

TABLE I. Parameters used for elastic and inelastic scattering calculations.

L^π	Reactions	E_x (MeV)	BEL (e^2b^L)	β	V_0 (MeV)	r_0 (fm)	a_0 (fm)	W_D (MeV)	W_S (MeV)	r'_0 (fm)	a'_0 (fm)	r_c (fm)
3^-	$^{208}\text{Pb}(\alpha, \alpha')^{208}\text{Pb}$	2.614	0.580	1.08	100.4	1.444	0.542	0.0	44.3	1.20	0.40	1.20
2^+	$^{152}\text{Sm}(\alpha, \alpha')^{152}\text{Sm}$	0.122	3.460	0.22	45.0	1.49	0.605	11.2	0.0	1.49	0.605	1.20
4^+	$^{152}\text{Sm}(\alpha, \alpha')^{152}\text{Sm}$	0.367	0.137	0.04	45.0	1.49	0.605	11.2	0.0	1.49	0.605	1.20
2^+	$^{234}\text{U}(\alpha, \alpha')^{234}\text{U}$	0.044	10.9	0.22	100.4	1.444	0.542	0.0	44.3	1.20	0.40	1.20
4^+	$^{234}\text{U}(\alpha, \alpha')^{234}\text{U}$	0.143	1.96	0.12	100.4	1.444	0.542	0.0	44.3	1.20	0.40	1.20

change the reflection coefficients and this may well not be compensated by a change of V or R .

III. TYPICAL RESULTS

In this section we illustrate the typical effects of the nuclear force at low energies and how Coulomb excitation experiments might be influenced. We chose as our examples calculations at a lab-

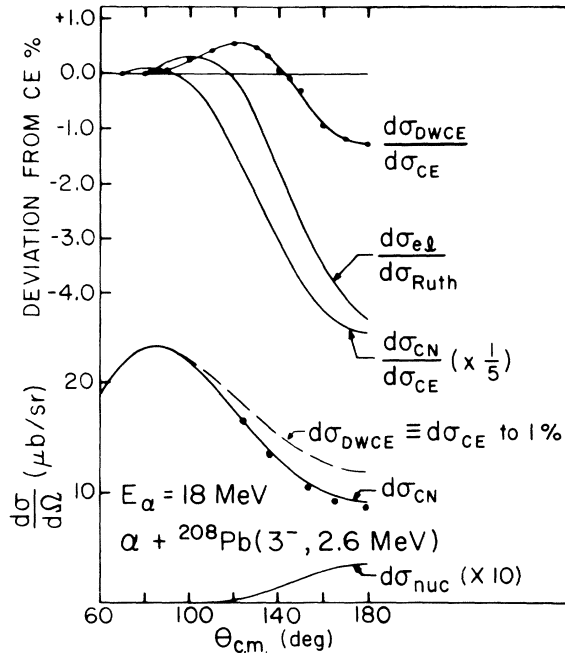


FIG. 3. Elastic and inelastic $E3$ Coulomb nuclear interference calculations for $\alpha + ^{208}\text{Pb}$ at 18 MeV. The lower curves show the angular distributions of the inelastic scattering assuming pure Coulomb excitation, distorted-wave Coulomb excitation, pure nuclear excitation (which is weak), and the complete interference. Several MeV below a Coulomb barrier defined by $1.3(A_1^{1/3} + A_2^{1/3})$ there is still an 18% interference effect. The points are the predictions of expression (13). The upper curves show the elastic ratio to Rutherford scattering (i.e., pure CE) and also the ratio to CE of the interference cross section and the DWCE cross section. We note that these angular distributions are different in form, contrary to what is assumed in semiclassical theories (e.g., Ref. 16).

oratory bombarding energy of 18 MeV on the three nuclei involved. The details of the potentials used are given in Table I. For the case of ^{152}Sm the barrier is about 16 MeV and we expect strong effects, but for ^{208}Pb and ^{234}U it would seem that the incident energy would be comfortably below the barrier which lies at $E_{\text{lab}} = 21.0$ MeV for Pb. Nevertheless, the elastic scattering data of Barnett and Phillips²¹ at 18 MeV show a few percent deviation from Rutherford values near $\theta = 180^\circ$. Note that the fits to these data in Ref. 21 for Pb were illustrative only and in fact are somewhat in error for the potentials given. The calculations were only taken to a matching radius of 12.5 fm owing to the use of a "universal" value $R + 8a$ in the program. Such an expression is more suited to proton scattering. A similar error was made in the calculations for Fig. 8 of Ref. 21 with the result that the cross section $d\sigma_n$ was underestimated. The optical potentials in this reference should be disregarded (see instead Ref. 38).

A. Elastic and inelastic scattering angular distributions

The calculations shown in Fig. 3 are the $L = 3$ results for ^{208}Pb which illustrate that the nuclear influence is also being felt in the inelastic channel (despite the plausible arguments put forward in Ref. 21) up to 22% at back angles. The solid points in Fig. 3, obtained as described in the next paragraph, give an adequate estimate of the complete calculation.

We can in general write the Coulomb nuclear interference cross section as

$$d\sigma_{\text{CN}} = |e^{i\phi} d\sigma_{\text{DWCE}}^{1/2} - d\sigma_{\text{nuc}}^{1/2}|^2, \quad (12)$$

where $d\sigma_{\text{DWCE}}$ is the cross section for "distorted-wave Coulomb excitation" and the angle ϕ describes the phase difference between the two amplitudes (and has no deeper significance, although it can be estimated by various semiclassical approximations¹⁴). The DWCE cross section²⁶ is that due to a process where nuclear-distorted waves are used together with a pure CE form factor; it is, we feel, the appropriate cross section with which to describe "pure Coulomb excitation" when nu-

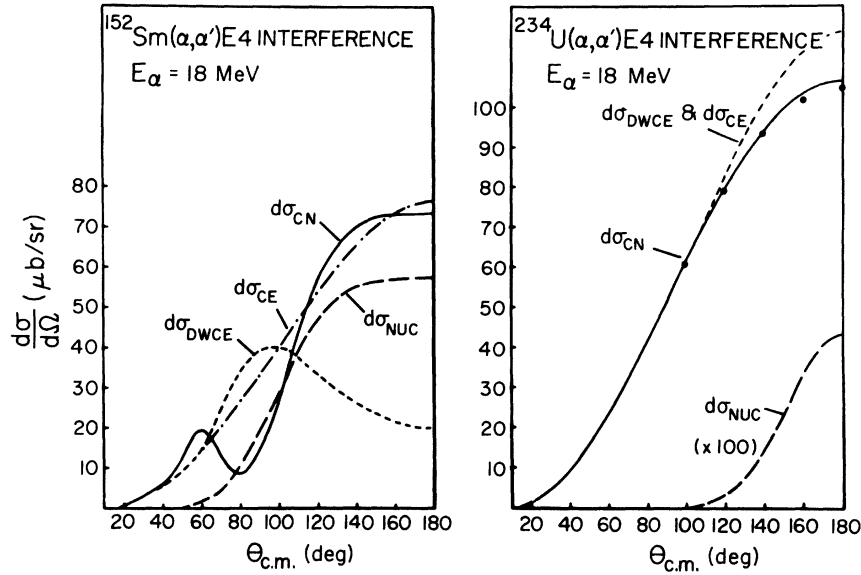


FIG. 4. Plots of the differential cross sections for $d\sigma_{\text{DWCE}}$, $d\sigma_{\text{CE}}$, $d\sigma_{\text{CN}}$, and $d\sigma_{\text{nuc}}$ versus $\theta_{c.m.}$. For (a) the reaction is as indicated, $^{152}\text{Sm}(\alpha, \alpha')^{152}\text{Sm}(0^+ \rightarrow 4^+)$, and for (b) it is $^{234}\text{U}(\alpha, \alpha')^{234}\text{U}(0^+ \rightarrow 4^+)$. All the parameters used in these calculations are given in Table I. The incident α lab energy is 18 MeV.

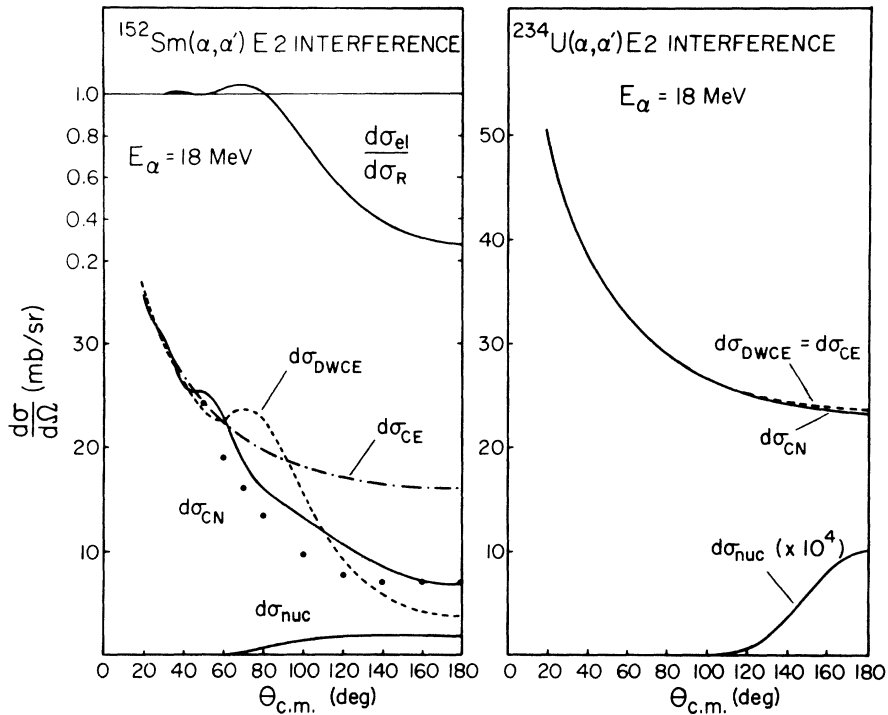


FIG. 5. Plots of the differential cross sections for $d\sigma_{\text{DWCE}}$, $d\sigma_{\text{CE}}$, $d\sigma_{\text{CN}}$, and $d\sigma_{\text{nuc}}$ versus $\theta_{c.m.}$. For (a) the reaction is $^{152}\text{Sm}(\alpha, \alpha')^{152}\text{Sm}(0^+ \rightarrow 2^+)$, and for (b) it is $^{234}\text{U}(\alpha, \alpha')^{234}\text{U}(0^+ \rightarrow 2^+)$. All the parameters used in these calculations are given in Table I. The ratio of the elastic scattering cross section of α on ^{152}Sm to the Rutherford scattering cross section is also plotted in (a). No such ratio is given for (b) because it is trivially unity for all $\theta_{c.m.}$. The incident α lab incident energy is 18 MeV for these calculations.

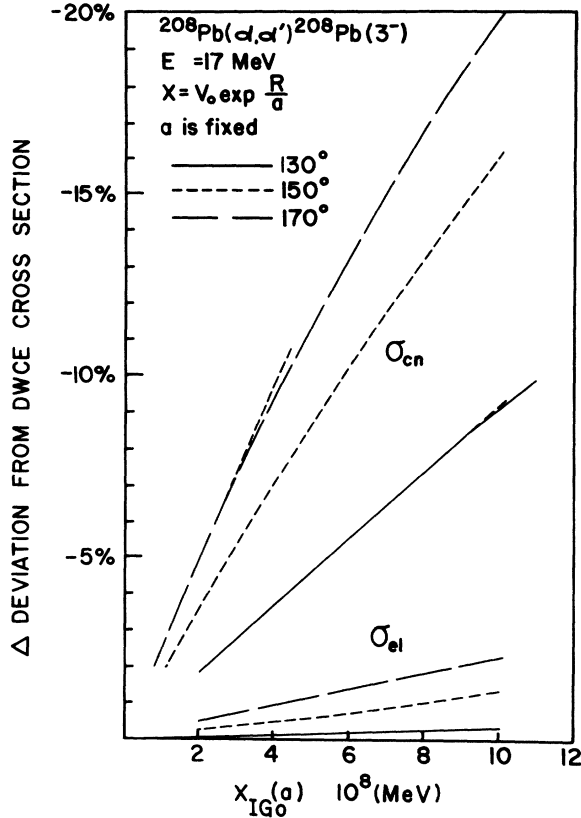


FIG. 6. Plot of the deviation of Δ of $d\sigma_{CN}$ from $d\sigma_{DWCE}$ [$(d\sigma_{CN} - d\sigma_{DWCE})/d\sigma_{DWCE}$ expressed in percent] as a function of the X_{Igo} for the $\alpha + {}^{152}\text{Sm}$ system. The variation of X_{Igo} is achieved by keeping a as a constant. Both the deviations of the elastic and inelastic ($L=2, 4$) cross sections are plotted. The incident α lab energy is 13 MeV in these calculations.

clear distortion is present, and its use can be sensibly extended well beyond the barrier (see Figs. 4 and 5 for example). To use pure CE cross sections in such regions is physically unreasonable and may produce incorrect deductions although it is true that their use may serve as a convenient normalization.⁵⁻⁷ Naturally, as the energy is decreased $d\sigma_{DWCE}$ becomes equal to $d\sigma_{CE}$, so that in our range the difference are quite insignificant and, furthermore, ϕ tends to zero. Thus we can obtain¹⁵ an excellent estimate of the interference simply by using

$$d\sigma_{CN} = |d\sigma_{CE}^{1/2} - d\sigma_{nuc}^{1/2}|^2, \quad (13)$$

where $d\sigma_{CE}$ comes from the semiclassical estimate and $d\sigma_{nuc}$ from a simple DWBA calculation (using Coulomb waves in fact). Since $d\sigma_{nuc}^{1/2}$ is directly proportional to $3\beta_L^N R_0 a^{-1} V_0 e^{R_0/a}$ in the DWBA, we see that when $d\sigma_{nuc}$ is small, when plotted as a function of $X_{Igo}(a)$ and of $\beta_L^N R_0$, a linear departure from the pure CE is expected (and indeed appears

in Figs. 6 and 8). Equation (13) was used to generate the solid points of Fig. 3.

We digress to remark that the presence of such a strong interference effect (which with hindsight we now recognize to be typical) must be allowed for in the interpretation of the reorientation measurements of Barnett and Phillips.²¹ The precise magnitude of the effect depends on the details of the form factors chosen and on other refinements of the calculations. A detailed reanalysis is in progress³⁸ which will probably show that the value of $B(E3)\dagger$ will rise from $0.58 \pm 0.04 e^2 b^3$ to about $0.60 \pm 0.04 e^2 b^3$, and that the quoted value of Q is a generous overestimate. However, the serious problem remains of obtaining a reliable ${}^{16}\text{O}$ -Pb nuclear potential at low energies (69 MeV) in order to evaluate possible nuclear effects in that part of the experiments of Ref. 21.

The $L=4$ results for ${}^{152}\text{Sm}$ and for ${}^{234}\text{U}$ are displayed in Fig. 4 and the effect of the barrier is most strikingly revealed in their comparison. For uranium a small deviation from Rutherford scattering is predicted (0.2% at $\theta_{c.m.} = 150^\circ$) and a deviation of the direct part of the $E4$ excitation of 6% from the pure CE value, whereas the samarium results are highly complex, which indicates a much stronger interaction with the barrier. Because the curve oscillates it is possible to find several angles at which the complete interference results in the same cross section as does the pure CE.

This is not the case for the $L=2$ Sm curve, which appears in Fig. 5. There, after an initial flourish around 60° the value of $d\sigma_{CN}$ drops steadily below the pure CE value. The solid points, the estimate of Eq. (13), again serve to illustrate the probable size of the nuclear effect. We notice here, for the samarium case, that the effect of nuclear distortion is too strong for Eq. (13) to be valid. For uranium (Fig. 5) the effect is a decrease of 0.9% from the values of $d\sigma_{DWCE}$ (and $d\sigma_{CE}$) at 105° . In the experiments of Bemis *et al.*²⁰ such a correction might be of great significance, for the $BE2$ values themselves were determined to $\pm 1\%$ and these directly determine the $BE4$ values by a subtraction technique. The amount of direct $E4$ yield to be attributed to the matrix element $\langle 4||M(E4)||0\rangle$ is also influenced by the 6% nuclear interference (Fig. 4). Nuclear interference in the double $E2$ excitation, which is the main contribution to the population of the 4^+ state, may also be significant, but requires a second-order or a coupled-channels⁵ code to evaluate. Our conclusions must be, given the nuclear potential⁶ and the stated choice of form factor, that 18 and 19 MeV are unsafe energies for CE at this level of precision (see Sec. VI and Fig. 12). Nuclear

corrections can be allowed for, however, if the nuclear potential information is reliable; admittedly this is a large if. Bemis *et al.*⁶ chose to work at 16 and 17 MeV for their final data and the corrections here are much less important.

Some general statements can be made concerning the alterations to the shape of the angular distributions at low levels of nuclear absorption. These features are borne out by specific calculations.

Figures 3–5 make evident the characteristic peaking at backward directions that is displayed by nuclear excitation. The form of the matrix element associated with this excitation, in fact, relates closely to what is found in sub-Coulomb transfer reactions. The main difference is that the form factor in the latter case falls off as $\exp(-\chi r)$ at large distances where $\chi = (2m B_n \hbar^{-2})^{1/2}$ and B_n is the separation energy of the transferred nucleon. This falloff is much slower than what is exhibited by $F_L^N(r)$. A crude estimate following Lemmer's treatment³⁹ shows that $d\sigma_{\text{nuc}}$ depends on $\exp[-d(\pi)a^{-1}(1 + \csc \frac{1}{2}\theta)]$. The dispersion about 180° directly relates to the a^{-1} falloff in $F_L^N(r)$. The nuclear effect in Coulomb excitation is therefore more confined about the region near 180° than in the case of nucleon transfer because a^{-1} is characteristically greater than χ . Furthermore, the dispersion is L independent. This is known to be the case in sub-Coulomb stripping⁴⁰ and it is evident in our calculations.

Although the shape of $d\sigma_{\text{nuc}}$ is L independent, the magnitude does indeed depend on the L transfer. To understand this, we refer to the article by Alder *et al.*,¹ where the dependence of $d\sigma_{\text{CE}}$ on ξ and L is exhibited. Excitations of the $E2$ type show a rapid rise to some peak value at small angles and this is followed by a slow descent to about half the peak value at 180° . The peak angle increases with ξ , being zero for $\xi = 0$, near 20° for $\xi = 0.2$, and near 120° when $\xi = 4.0$. The situation is somewhat different for L greater than 2. The angular distribution for $\xi < 0.5$ shows for $L = 3$ a gentle rise from 0° to 180° . The rise is more rapid but confined to larger angles if L is increased. The nuclear effect, in such instances, can only alter the peak value at 180° . If ξ is increased beyond 0.5 the peaking becomes more evident near 90° . For all L values the nuclear effect only quickens the falloff near the backward direction.

With increasing energy, $d\sigma_{\text{nuc}}$ shows broad dispersion and this is evident in Fig. 5 on the case of ^{152}Sm . At even higher energies $d\sigma_{\text{nuc}}$ peaks at some grazing angle and this is usually seen also in $d\sigma_{\text{CN}}$. Beyond the grazing angle, the two modes of excitation become nearly equal and tend to can-

cel each other. There then appears a characteristic broad minimum, clearly seen for example, in the case of the scattering by ^{208}Pb at 22 MeV, as is shown in Ref. 15.

IV. NUCLEAR EFFECTS FOR THE REACTION

$$^{152}\text{Sm}(\alpha, \alpha')^{152}\text{Sm}(2^+, 4^+)$$

There has been recent experimental and theoretical work⁵ on (α, α') to the 2^+ and 4^+ states of ^{152}Sm , which lie at 122 and 367 keV at bombarding energies both below and in the region of the Coulomb barrier. The study has also been extended⁵ to other rare-earth nuclei ^{154}Sm and ^{186}S . Similar work on the targets ^{154}Sm , ^{166}Er , and ^{182}W has been reported.⁶ Also, there is a recent study²³ of ^{168}Er and $^{184, 186}\text{W}$. Inasmuch as our calculations do not include higher static or dynamic moments our general results will apply equally to all these nuclei, after the appropriate change in $E_{\text{c.m.}}$ and E_{barrier} and the different excitation energies are made.

We adopt the four-parameter optical potential used in Ref. 5 (see Table I). All the input parameters are listed in Table I. The results of the calculations at $E_\alpha = 13$ MeV are shown in Fig. 6 in which are plotted the (negative) percentage deviations of $d\sigma_{\text{CN}}$ from $d\sigma_{\text{DWCE}}$ (identical to $d\sigma_{\text{CE}}$ at this energy) as a function of the nuclear strength as measured by X_{Igo} . Three sets of curves are presented, for elastic scattering, for 2^+ inelastic scattering, and for 4^+ inelastic scattering, and each comprises results at 170° , 150° , and 130° . Values of $X_{\text{Igo}}(a)$ were obtained by varying V and R at constant diffusenesses a , and values appropriate to the potential set used in Table I occur at $X_{\text{Igo}}(a) = 2.3 \times 10^7$ MeV.

As well as the expected linear variation with strength of the nuclear tail, we find in Fig. 6 another characteristic result of low-energy Coulomb-nuclear interference. The sensitivity to multipolarity is quite marked, with the direct $E4$ cross section deviating by 7% when the $E2$ cross section deviates by 2%, and the elastic cross section by somewhat less than 1% from the DWCE (or pure CE) values. We understand that the difference between $L = 2$ and $L = 4$ as a direct consequence of the L dependence of the radial form factor r^{-L-1} which for $L = 4$ is much shorter range and thus competes more with the nuclear effect.

The inelastic scattering is influenced by two aspects of the nuclear effects; one is that the radial wave functions are modified and the other is that in addition to the Coulomb form factor a nuclear form factor appears in the matrix element. The effect of the change in the radial wave functions is nearly the same for elastic and in-

elastic scattering but the effect of the nuclear form factor is very pronounced. In fact, the nuclear form factor produces essentially all the deviation at this energy range. Thus the inelastic cross section $d\sigma_{CN}$ becomes a measure of the nuclear form factor and we may conclude that if an optical potential overestimates the experimental elastic deviation from Rutherford scattering, it will certainly overestimate the interference effect in $d\sigma_{CN}$.

In Fig. 7 the results of varying the quantity $X_{Igo}(a)$ for the imaginary potential are given. In this case the radius R was held constant and the strength W_v was varied over the range 3–30 MeV. The general effect is that the nuclear effect is enhanced as W_v is decreased because less flux is absorbed. The effects are greatest for a case such as this where the real and imaginary wells have the same geometry; for Pb and U we shall use smaller imaginary wells and the effect of their variation will be less.

The results given in the next figure, Fig. 8, are those most directly relating to the question of the safe energy for inelastic scattering. We plot, for three angles, the negative deviation (Δ) of the cross section from the DWCE value for elastic scattering, and for inelastic scattering to the 2^+ and 4^+ states. The same characteristics seen in Fig. 6 at a single energy are now apparent over the whole energy range of 11–15 MeV; the 4^+ de-

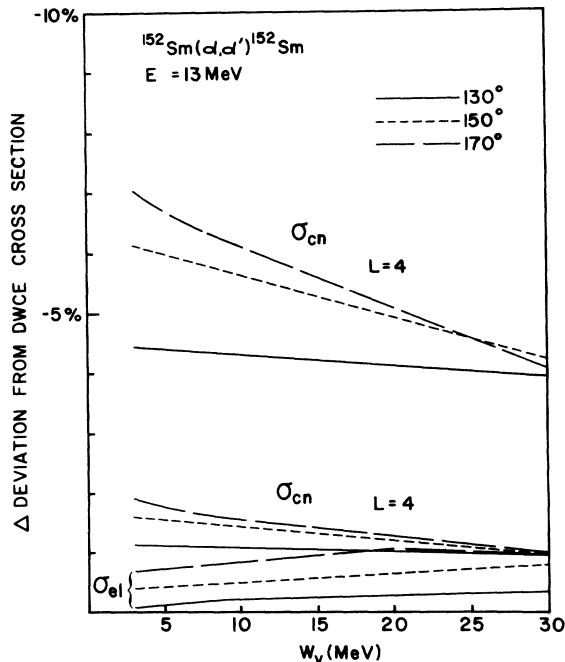


FIG. 7. Plot of the deviation Δ of $d\sigma_{CN}$ from the $d\sigma_{DWCE}$ as a function of the imaginary potential strength W_v for the $\alpha + {}^{152}\text{Sm}$ reaction at a lab energy of 13 MeV.

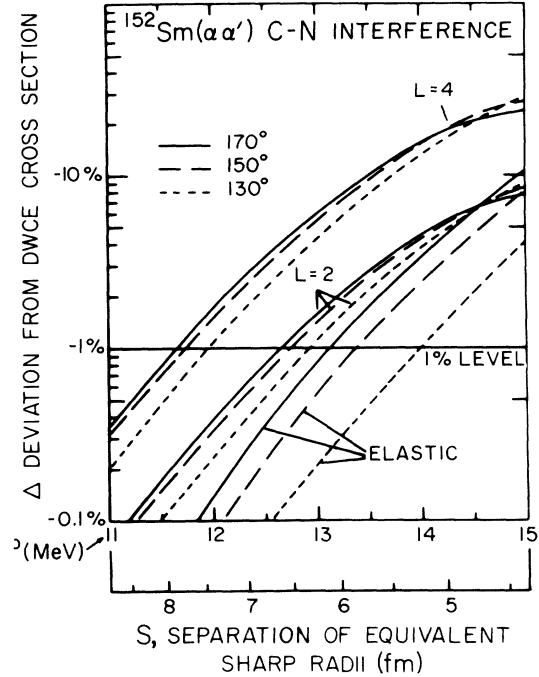


FIG. 8. (α, α') and (α, α) Coulomb nuclear interference effects for the $L=2$ and $L=4$ transition in ${}^{152}\text{Sm}$ as a function of energy. Results for three angles (170° , 150° , 130°) are given. The important feature is the magnification effect resulting in the $L=2$ deviation due to the interference exceeding the elastic scattering deviations and the $L=4$ deviations considerably exceeding those for $L=2$. The distance scale is defined in Eq. (15).

viation (for the direct part of the cross section) is much larger than the 2^+ deviation, which itself is generally larger than the elastic deviation. The 1% deviation level is indicated on the figure and we see that an energy of 12.6 MeV will result in this effect on $d\sigma_{2^+}(170^\circ)$ and a 4% effect on $d\sigma_{4^+}(170^\circ)$. The corresponding influence of nuclear effects on the elastic scattering, $d\sigma_{el}(170^\circ)$ is $\frac{1}{2}\%$.

A second abscissa on Fig. 7 gives the value of the quantity S , defined in Eq. (1). In order to make sensible comparisons with other pairs of ions we must try and use for r_0 a value is not merely phenomenological or arbitrary. Thus we should avoid choosing a value corresponding to the radius of the potential well which describes elastic or inelastic scattering because at these low energies the consequence of the Igo ambiguity is that such radii are uncertain to 15–20% (see Sec. IIB). We should also avoid choosing an interaction radius which corresponds to the peak of the Coulomb plus nuclear barrier, since this also depends on the potential parameters (although quite weakly, it is true). To this end, we adopt the approach detailed by Myers⁴¹ and consider as the fundamental quantity of interest the equivalent

sharp radius (ESR) of the nuclear density distribution, taking it to be the same for the neutron and proton density distributions and equal to

$$R_p = R_n = R = 1.13A^{1/3} \quad (14)$$

from the experiments analyzed in Ref. 41. It is this radius which we will expect to vary as $A^{1/3}$ as shown; other quantities, such as the halfway radius or the mean-square radius, can be derived from it. Our distance scale is then the measure of the separation of the equivalent sharp radii of the two nuclei and is given by

$$S = Z_1 Z_2 e^2 E_{c.m.}^{-1} - 1.13(A_1^{1/3} + A_2^{1/3}). \quad (15)$$

(Light nuclear projectiles, including the α particle, are generally not leptodermous,⁴¹ but we assume the correction for this fact is small.) This choice of distance scale shows the $E_\alpha = 12.6$ MeV corresponds to $S = 6.7$ fm and at this point we still have to contend with a 1% effect. At $E_\alpha = 11$ MeV, $S = 8.8$ fm ($\theta = 170^\circ$), our values are $\Delta_{el} < 0.01\%$, $\Delta_{2^+} = 0.07\%$, and $\Delta_{4^+} = 0.36\%$, which is the energy where Bruckner *et al.*⁵ analyze their results in terms of pure CE theory.

The precise numerical values we have given for Δ_i depend on the assumptions made about both the optical potential which is used to generate the form factor and the deformation parameter which multiplies it; corrections made to CE data must bear this in mind. The optical potential is not very energy dependent and so can be obtained at higher energies.

V. NUCLEAR EFFECTS FOR THE REACTION $^{208}\text{Pb}(\alpha, \alpha')^{208}\text{Pb}(3^-)$

The results for the case of the octupole state in ^{208}Pb follow a similar pattern to those of the previous section. Figure 9 demonstrates the linear dependence of the quantities Δ on $X_{Igo}(a)$ for a constant diffuseness at an energy of 17 MeV. The potential chosen was one (Set B) determined by Barnett and Lilley (see Table I) in their recent extensive work³⁴ on α -scattering and reaction cross sections on ^{208}Pb and ^{209}Bi . Global fits at a variety of energies and value of X_{Igo} is 7.2×10^7 MeV, and at 17 MeV $\Delta_{el} = 1.5\%$ while $\Delta_{3^-} = 14.8\%$, both at $\theta = 170^\circ$.

Figure 10 displays the results of the calculations as a function of energy and of the distance S between the equivalent sharp radii. At $\theta = 170^\circ$ the deviation $\Delta_{3^-} = 1\%$ occurs at 15.2 MeV and corresponds to $S = 7.3$ fm; the elastic value Δ_{el} is only 0.1% at this energy. The assumption in Ref. 21 that nuclear effects were negligible at 17.5 and 18 MeV is now recognized to be in error, which demands a reevaluation³⁸ of the BE3 and the Q, as was discussed in Sec. IIIA. There are

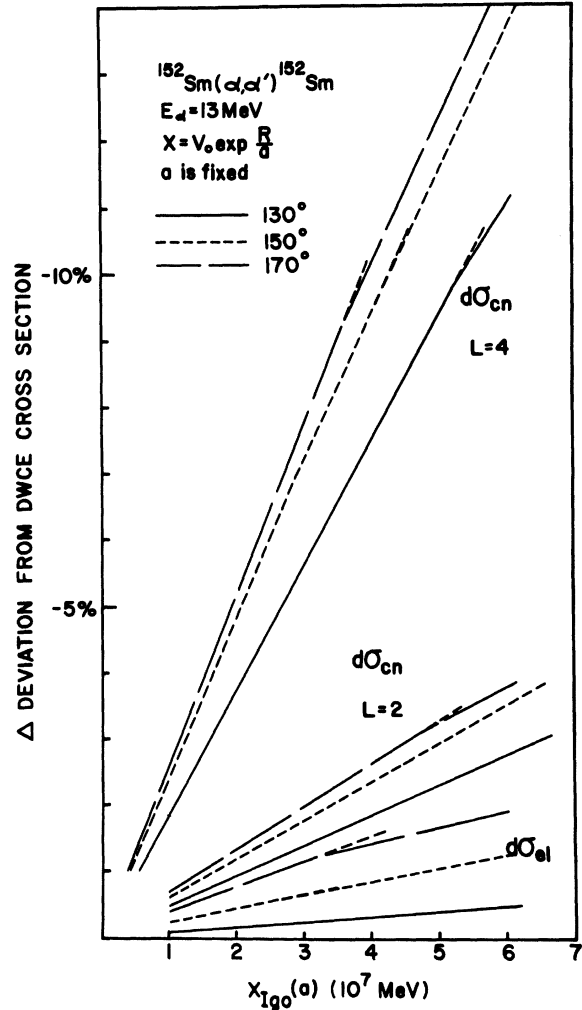


FIG. 9. A similar plot of Δ versus X_{Igo} (as in Fig. 6) for $\alpha + ^{208}\text{Pb}$ at a lab energy of 17 MeV.

strong effects even at $E_\alpha = 16$ MeV for the (α, α') cross section and several studies have assumed pure CE at this energy.⁴² The nuclear effects are strong in the lead case probably because the CE cross sections are so low (due to the higher multipolarity and to the very high excitation energy of the 3^- state).

VI. NUCLEAR EFFECTS FOR THE REACTION $^{234}\text{U}(\alpha, \alpha')^{234}\text{U}(2^-, 4^+)$

As has been foreshadowed in earlier sections, the results for uranium conform closely to the trend of those of samarium. The deviations Δ_i as functions of $X_{Igo}(a)$ (with constant diffuseness) at 18 MeV closely resemble those in Fig. 6 and thus will not be displayed here.

The curves for estimating the safety of a given bombarding energy are in Fig. 11. A 1% de-

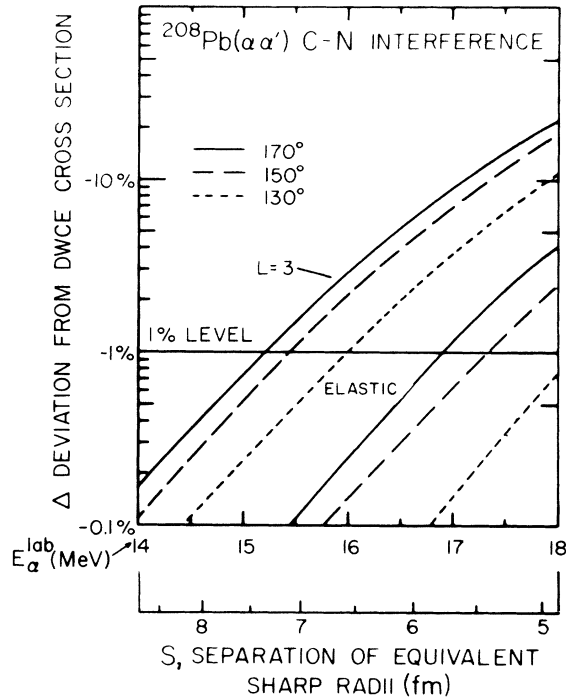


FIG. 10. $L=3$ excitations in ^{208}Pb with α particles as a function of bombarding energy. The sensitivity to nuclear effects is much greater for inelastic scattering than for elastic scattering and is a strong function of multipolarity (see Figs. 8 and 11).

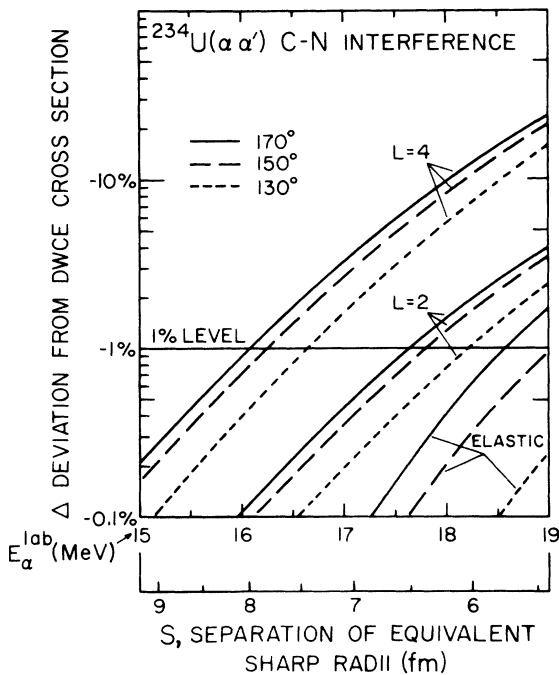


FIG. 11. Interference effects for $L=2, 4$ excitations in ^{234}U as a function of α energy. See Figs. 8 and 10.

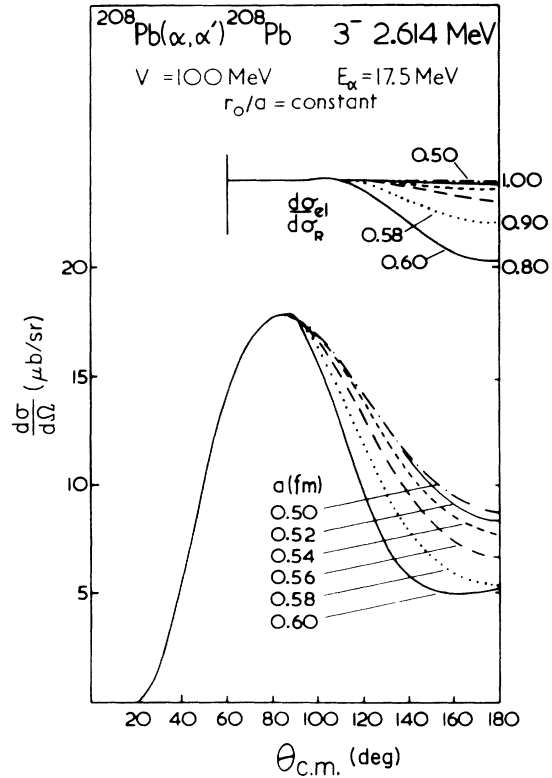


FIG. 12. Plot of $d\sigma_{\text{CN}}$ and $d\sigma_{\text{el}}/d\sigma_{\text{Ruth}}$ for various diffusenesses a with r_0/a kept as a constant. The incident α energy is 17 MeV.

viation for $L=2$ and $\theta=150^\circ$ occurs at $E_\alpha=17.7$ MeV and $S=6.2$ fm, while the direct $E4$ term has $\Delta_{\alpha^+}=6\%$ and the elastic has $\Delta_{\text{el}}=0.1\%$. It may well be that for a permanently deformed system such as ^{234}U the static moments will also influence both the barrier and the details of Fig. 11. Experimental evidence for these effects comes from the (α, α') work of Bemis *et al.* (Ref. 20 and Sec. IIIA), where deviations at the 1–2% level from the pure $E2$ excitation are observed at 19 and 19.5 MeV, and also in the (α, α') and total reaction cross section results of Freiesleben and Hui-zenga⁴³ at higher energies. These latter authors show that the effects of permanent deformation are quite small; for example, their σ_{total} results for the deformed nucleus ^{234}U have the same relative energy dependence as the results of Barnett and Lilley³¹ for the spherical nuclei ^{208}Pb and ^{209}Bi . The effects can be expected to be more pronounced in the α' channel and detailed attempts are being made⁴⁴ to find methods of calculating with suitably deformed potentials.

VII. IGO AMBIGUITY AS A FUNCTION OF DIFFUSENESS

We now examine briefly how the quantity $X_{\text{Igo}}(a) = V_0 e^{R/a}$ may depend on the diffuseness of the po-

tential for the same scattering predictions; it is a constant, for example, for constant values of R/a , but such a relationship between R and a does *not* lead to identical predictions since the form factor also depends on $e^{-r/a}$. We illustrate this feature in Fig. 12 for both elastic and inelastic scattering of α particles on ^{208}Pb for a wide range of a -values, with R/a held constant. The effects of the interaction become stronger as the size of the real potential grows (the volume integral is proportional to a^3). It is important to realize that the potentials defined in Fig. 12 have the same magnitude at the halfway radius R where, as discussed in Sec. IIB, they should have the same value at a point in the surface R_s in order to be equivalent. For elastic scattering the constant quantity is just this value of the real potential at R_s , namely

$$V(R_s) \equiv X_{\text{Igo}} \equiv V_0 e^{R/a} e^{-R_s/a}. \quad (10)$$

For the case of the inelastic scattering of strongly absorbed particles we may expect the *equivalent form factors are those whose magnitude in the surface is the same when the diffuseness is changed*. Although we shall choose the surface point to be defined by $r = R_s$ it may be that a slightly different point gives a better invariant. Numerous surface radii can be defined, depending on the analysis, especially at high energies, and in Ref. 35, six such radii were discussed. The full statement of the Igo ambiguity for inelastic scattering would then become

$$(\beta R) a^{-1} V(R_s) = (\beta R) a^{-1} X_{\text{Igo}} = \text{constant}. \quad (16)$$

This leads to the prediction that for equivalent form factors the deformation length $\delta = \beta R$ must scale as the diffuseness; consequently the deformation length can only be determined once the diffuseness has been chosen, following which a choice of R finally enables a value for β to be extracted from the fit to the data.

We have made tests of these ideas with encouraging results. It is important to realize that these ideas will work best for potentials in which the imaginary part is weak in the surface region compared to the real part. The potentials do not need to have the same geometry.

We can conclude that just as Eq. (10) provides a suitable invariant for reasonable changes of V_0 and R and a for elastic scattering, so it is likely that Eq. (16) does also for inelastic scattering.

VIII. CONCLUSIONS

We have employed the DWBA code PATIWEN,⁶ which can sum over a large number of partial

waves with adequate radial integration, to investigate the onset of nuclear effects in the Coulomb excitation regime below the Coulomb barrier. We find these effects to be large, to be dependent on the multipolarity of the transition, and to be strongly enhanced over the elastic scattering deviations from the Rutherford value. Our results for $\alpha + \text{sm}$, U ($L = 2, 4$) and for $\alpha + \text{Pb}$ ($L = 3$) are summarized in Figs. 8, 10, and 11. From these curves an estimate of "safe energy", or a "safe distance" between the equivalent sharp radii, for a given percentage effect can be made. A noteworthy feature is that the energy variation of each curve is very similar: the percentage deviations from DWCE cross sections increase by nearly a factor of 10 for an α particle incident energy increment of 1.6 MeV. We have also shown that in this energy range a reliable estimate of the Coulomb-nuclear interference can be made from a simple expression [Eq. (13)].

The results are interpreted in terms of generalized Igo ambiguities for elastic and inelastic scattering [Eqs. (10) and (16), respectively] which we derive from the known constancy of equivalent potentials in the surface region. These ambiguities have been demonstrated in preliminary calculations for inelastic scattering, once the elastic potential is fixed; the results only determined $(\beta r)/a$ and so, even to obtain the deformation length $\delta = R$, the value of the diffuseness must be determined. At low energies such as these, however, values of the diffuseness differing by 10% and of values of R differing by as much as 20% can be found to fit the data. Extreme caution is warranted, therefore, in trying to determine quantities βR or β which are then to be related to the nuclear deformation, for very little is known of the optical potential at low energies.

ACKNOWLEDGMENTS

Two of us (ARB and DHF) are grateful to the Science Research Council's Daresbury Laboratory for the use of their excellent IBM 370/165 computing facility where most of these calculations were done. It is a pleasure for one of us (DHF) to thank Professor Taro Tamura, Professor Takeshi Udagawa, Professor John Lilley, and Professor Richard Fuller for many illuminating and fruitful discussions on various occasions. Finally, useful discussions with Professor G. Rawitscher are gratefully acknowledged.

- *Work supported by the U. S. Energy Research and Development Administration and the U. K. Science Research Council.
- †Part of the work was done while the author was a SRC research fellow at the Department of Theoretical Physics, University of Manchester.
- ¹K. Alder, A. Bohr, T. Huus, B. Mottleson, and A. Winther, *Rev. Mod. Phys.* **28**, 432 (1956).
- ²L. C. Biedenharn and P. J. Brussard, *Coulomb Excitation* (Clarendon, Oxford, 1965).
- ³K. Alder and A. Winther, *Electromagnetic Excitation* (North-Holland, Amsterdam, 1974).
- ⁴J. de Boer and J. Eichler, in *Advances in Nuclear Physics*, edited by M. Baranger and E. Vogt (Plenum, New York, 1968), Vol. 1, p. 1.
- ⁵W. Bruckner, J. G. Merdinger, D. Pelte, U. Smilansky, and K. Traxel, *Phys. Rev. Lett.* **30**, 57 (1973); W. Bruckner, D. Husar, D. Pelte, K. Traxel, M. Samuel, and U. Smilansky, *Nucl. Phys.* **A231**, 159 (1974).
- ⁶C. E. Bemis, P. H. Stelson, F. K. McGowen, W. T. Milner, J. L. C. Ford, R. L. Robinson, and W. Tuttle, *Phys. Rev. C* **8**, 1934 (1973).
- ⁷T. K. Saylor, J. X. Saladin, I. Y. Lee, and K. A. Erb, *Phys. Lett.* **42B**, 51 (1972); K. A. Erb, J. E. Holden, I. Y. Lee, J. X. Saladin, and T. K. Saylor, *Phys. Rev. Lett.* **29**, 1010 (1972); I. Y. Lee, J. X. Saladin, C. Baklash, J. E. Holden, and J. O'Brien, *ibid.* **33**, 383 (1974); F. Rosel, J. X. Saladin, and K. Alder, *Comp. Phys. Commun.* **8**, 35 (1974).
- ⁸A. H. Shaw and J. S. Greenberg, *Phys. Rev. C* **10**, 263 (1974).
- ⁹D. Cline, H. S. Gertzman, H. E. Gove, P. M. S. Lesser, and J. J. Schwartz, *Nucl. Phys.* **A133**, 445 (1969).
- ¹⁰P. M. S. Lesser, D. Cline, P. Goode, and R. N. Koroshki, *Nucl. Phys.* **A180**, 597 (1972).
- ¹¹J. A. Thomson, R. P. Scharenberg, and W. R. Lutz, *Phys. Rev. C* **4**, 1699 (1971).
- ¹²D. H. Feng and A. R. Barnett, *Comp. Phys. Commun.* (to be published).
- ¹³A. Winther and J. de Boer, in *Coulomb Excitation*, edited by K. Alder and A. Winther (Academic, New York, 1965), p. 303.
- ¹⁴R. A. Broglia, S. Landowne, and A. Winther, *Phys. Lett.* **40B**, 293 (1972); R. A. Broglia and A. Winther, *Phys. Rep. C* **4**, 155 (1972); *Nucl. Phys.* **A182**, 112 (1972).
- ¹⁵A. R. Barnett, D. H. Feng, and L. J. B. Goldfarb, *Phys. Lett.* **48B**, 290 (1973).
- ¹⁶F. D. Bacchetti, D. G. Kover, B. G. Harvey, J. Mahoney, B. Mayer, and F. G. Puhlhofer, *Phys. Rev. C* **6**, 2215 (1972).
- ¹⁷F. T. Baker and R. Tickle, *Phys. Rev. C* **5**, 544 (1972).
- ¹⁸E. E. Gross, H. G. Bingham, M. L. Halbert, D. C. Hensley, and M. H. Saltmarsh, *Phys. Rev. C* **10**, 45 (1972).
- ¹⁹J. C. L. Ford, K. S. Toth, D. C. Hensley, R. M. Gaedke, P. J. Liley, and S. T. Thornton, *Phys. Rev. C* **8**, 1466 (1973).
- ²⁰C. E. Bemis, F. K. McGowen, J. C. L. Ford, W. J. Milner, P. H. Stelson, and R. L. Robinson, *Phys. Rev. C* **8**, 1466 (1973).
- ²¹A. R. Barnett and W. R. Phillips, *Phys. Rev.* **186**, 1205 (1969).
- ²²F. S. Stephens, R. M. Diamond, N. K. Glendenning, and J. de Boer, *Phys. Rev. Lett.* **24**, 1137 (1970).
- ²³F. S. Stephens, R. M. Diamond, and J. de Boer, *Phys. Rev. Lett.* **28**, 1151 (1971).
- ²⁴A. R. Barnett, D. H. Feng, J. W. Steed, and L. J. B. Goldfarb, *Comp. Phys. Commun.* **8**, 377 (1974).
- ²⁵M. Samuel and U. Smilansky, *Comp. Phys. Commun.* **2**, 455 (1971).
- ²⁶R. H. Bassel, G. R. Satchler, R. M. Drisko, and E. Rost, *Phys. Rev.* **128**, 2693 (1962); E. Rost, *ibid.* **128**, 2708 (1962).
- ²⁷G. R. Satchler, *Nucl. Phys.* **77**, 481 (1966).
- ²⁸T. Tamura, *Rev. Mod. Phys.* **37**, 679 (1965).
- ²⁹D. H. Feng and A. R. Barnett (unpublished).
- ³⁰G. Igo, *Phys. Rev. Lett.* **1**, 72 (1958); *Phys. Rev.* **115**, 1665 (1959).
- ³¹M. E. Cage, A. J. Cole, and G. J. Pyle, *Nucl. Phys.* **A201**, 418 (1973).
- ³²D. F. Jackson and C. G. Morgan, *Phys. Rev.* **175**, 1402 (1968).
- ³³P. Mailandt, J. S. Lilley, and G. W. Greenlees, *Phys. Rev. C* **8**, 2189 (1973).
- ³⁴A. R. Barnett and J. S. Lilley, *Phys. Rev. C* **9**, 2010 (1974).
- ³⁵B. Fernandez and J. S. Blair, *Phys. Rev. C* **1**, 523 (1970).
- ³⁶G. H. Rawitscher, *Nucl. Phys.* **83**, 259 (1966).
- ³⁷A. R. Barnett, D. H. Feng, and L. J. B. Goldfarb, in *Proceedings of the International Conference on Nuclear Structure and Spectroscopy, Amsterdam, Holland, 1974*, edited by H. P. Blok and A. E. L. Dieperink (Scholar's Press, Amsterdam, 1974).
- ³⁸A. R. Barnett and J. Lowe (unpublished).
- ³⁹R. H. Lemmer, *Nucl. Phys.* **39**, 680 (1962).
- ⁴⁰M. Dost, W. R. Herring, and W. R. Smith, *Nucl. Phys.* **A93**, 357 (1967).
- ⁴¹W. D. Myers, *Nucl. Phys.* **A204**, 465 (1973).
- ⁴²E. Grosse, M. Dost, K. Haberkant, J. W. Hertel, H. V. Klapdor, H. J. Korner, D. Proetel, and P. Von Brentano, *Nucl. Phys.* **A174**, 525 (1971).
- ⁴³H. Freiesleben and J. R. Huizenga, *Nucl. Phys.* **A224**, 503 (1974).
- ⁴⁴J. Rasmussen *et al.*, in *Proceedings of the International Conference on Nuclear Physics, Munich, Germany, 1973*, edited by J. de Boer and H. J. Mang (North-Holland, Amsterdam/American Elsevier, New York, 1973), p. 351.